

Phase separation in a spin-orbit-coupled Bose-Einstein condensate

Sandeep Gautam* and S. K. Adhikari

Instituto de Física Teórica, Universidade Estadual Paulista (UNESP), 01.140-070 São Paulo, São Paulo, Brazil

(Received 8 August 2014; revised manuscript received 19 September 2014; published 20 October 2014)

We study a spin-orbit (SO)-coupled hyperfine spin-1 Bose-Einstein condensate (BEC) in a quasi-one-dimensional trap. For an SO-coupled BEC in a one-dimensional box, we show that in the absence of the Rabi term, any nonzero value of SO coupling will result in a phase separation among the components for a ferromagnetic BEC, like ^{87}Rb . On the other hand, SO coupling favors miscibility in a polar BEC, like ^{23}Na . In the presence of a harmonic trap, which favors miscibility, a ferromagnetic BEC phase separates, provided that the SO-coupling strength and number of atoms are greater than some critical value. The Rabi term favors miscibility irrespective of the nature of the spin interaction: ferromagnetic or polar.

DOI: [10.1103/PhysRevA.90.043619](https://doi.org/10.1103/PhysRevA.90.043619)

PACS number(s): 03.75.Mn, 03.75.Hh, 67.85.Bc, 67.85.Fg

I. INTRODUCTION

A Bose-Einstein condensate (BEC) with spin degrees of freedom, known as a spinor BEC, was first experimentally realized and studied in a gas of ^{23}Na atoms, with hyperfine spin $F = 1$, in an optical dipole trap [1]. This led to a flurry of investigation on both the theoretical and the experimental fronts, which has been reviewed in Ref. [2]. In the present work, we study the ground-state structure of the $F = 1$ spin-orbit (SO)-coupled spinor BEC in a quasi-one-dimensional (quasi-1D) trap [3] within the framework of the mean-field theory. The mean-field theory to study $F = 1$ spinor BECs was developed independently by Ohmi *et al.* [4] and Ho [5]. The SO interaction is absent in neutral atoms and engineering with an external electromagnetic field is needed for its experimental realization. A variety of SO couplings can be engineered by counterpropagating Raman lasers coupling the hyperfine states, and the parameters of this coupling can be controlled independently [6]. The SO interaction has been achieved recently with equal strengths of Rashba [7] and Dresselhaus [8,9] couplings employing a necessary engineering to obtain experimentally an SO-coupled BEC of two of the existing three hyperfine spin components of the $F = 1$ state of ^{87}Rb [10,11] forming a pseudospinor BEC. This was followed by other experiments on SO-coupled pseudospinor BECs [12]. In the case of an $F = 1$ spinor BEC, there are theoretical proposals to realize an SO-coupling interaction involving three hyperfine spin components [13]. SO-coupled degenerate Fermi gases (^{40}K and ^6Li) have also been experimentally realized [14]. A mean-field Gross-Pitaevskii (GP) equation for the theoretical study of dynamics in SO-coupled BECs has also been proposed [2,13,15,16].

The ground states of an SO-coupled two-component pseudo-spin-1/2 BEC and of a three-component spinor BEC have been theoretically investigated by Wang *et al.* [17]. It has further been established that SO-coupled spin-1/2 (pseudospinor), $F = 1$ and $F = 2$ spinor BECs in quasi-two-dimensional (quasi-2D) traps [3] can have a variety of nontrivial ground-state structures [18–20]. There have been studies on the intrinsic spin-Hall effect [21], chiral confinement [22], superfluidity [23], Josephson oscillation [24], vortices

[25], and solitons [26] in SO-coupled BECs. In general, for experimentally feasible parameters, the ground state of an $F = 1$ spinor BEC can host a single vortex or a square vortex lattice for weak and strong SO coupling, respectively [20]. Additionally, plane- and standing-wave states appear as ground states in the case of ferromagnetic and polar (antiferromagnetic) BECs, respectively, for medium strengths of SO coupling [20]. The ground state of the $F = 1$ spinor BEC in the presence of a homogeneous magnetic field has also been studied [27–29]. It was shown in Refs. [28] and [29] that a uniform magnetic field can lead to a phase separation in polar BEC. Phase separation has already been observed in a pseudospinor BEC consisting of two hyperfine states of ^{87}Rb in quasi-2D geometries [10].

In this paper, we investigate the ground state of an SO-coupled $F = 1$ spinor BEC in a quasi-1D trap. For the model of SO-coupling employed in this work, we find that, compared to a homogeneous magnetic field, SO coupling leads to a phase separation in the case of a ferromagnetic BEC, whereas in the case of a polar BEC, it makes the miscible profile energetically more stable. Here, we use a numerical solution of the generalized mean-field GP equation [15,16] to study the possible phase separation between the different hyperfine spin components of an SO-coupled BEC. We also study the possibility of a phase separation in a uniform spinor condensate in a 1D box employing an analytical model. The results of this analytical study provide a qualitative understanding of the numerical findings for a trapped SO-coupled BEC.

The paper is organized as follows. In Sec. II, we describe the coupled GP equation used to study the SO-coupled $F = 1$ spinor BEC in a quasi-1D trap. This is followed by an analytical investigation of an SO-coupled spinor BEC in a 1D box in Sec. III. By comparing the energies of various competing geometries for both ferromagnetic and polar BECs, the ground-state structure is determined from a minimization of energy. In the case of a mixture of two scalar BECs, similar analysis leads to the criterion for a phase separation [30]. In Sec. IV, we numerically study the SO-coupled spinor BEC in a quasi-1D trap. We conclude by providing a summary of this study in Sec. V.

II. MEAN-FIELD MODEL FOR AN SO-COUPLED BEC

For the electronic states of a hydrogen-like atom the SO contribution to the atomic spectrum naturally appears

*sandeepgautam24@gmail.com

because of the magnetic energy of this coupling existing due to electronic charge. In the case of the hyperfine states of neutral atoms, engineering with external electromagnetic fields is required for the SO coupling to contribute to the BEC. We use the SO-coupled interaction from the experiment by Lin *et al.* [10] for two hyperspin components of the ^{87}Rb hyperfine state $5S_{1/2}$, realized with strength γ using two counterpropagating Raman lasers of wavelength λ_r oriented at an angle β_r : $\gamma = \hbar k_r/m$, where $k_r = 2\pi \sin(\beta_r/2)/\lambda_r$ and m is the mass of an atom. This SO coupling is equivalent to that of an electronic system with equal contributions of Rashba [7] and Dresselhaus [8] couplings and with an external uniform magnetic field. However, here we consider the SO coupling among the three spin components of the $F = 1$ state, e.g., $|F = 1, m_F = 1\rangle$, $|F = 1, m_F = 0\rangle$, and $|F = 1, m_F = -1\rangle$, where m_F is the z projection of F . It has been shown [31] that this SO coupling among the three hyperfine spin components can be generated by engineering as in Ref. [10]. We consider the three spin components of the $F = 1$ hyperfine state $5S_{1/2}$ of ^{87}Rb and $3S_{1/2}$ of ^{23}Na .

We consider such a quasi-1D hyperfine spin-1 SO-coupled spinor BEC confined along the x axis obtained by making the trap along the y and z axes much stronger than that along the x axis. The transverse dynamics of the BEC is assumed to be frozen to the respective ground states of harmonic traps. Then the single-particle quasi-1D Hamiltonian of the system under the action of a strong transverse trap of angular frequencies ω_y and ω_z along the y and z directions, respectively, can be written as [10,32]

$$H_0 = \frac{p_x^2}{2m} + \gamma p_x \Sigma_z + \Omega \Sigma_x, \quad (1)$$

where $p_x = -i\hbar\partial_x$ is the momentum operator along the x axis, Ω is the Rabi frequency [10,11], and Σ_z and Σ_x are the matrix representations of the z and x components of the spin-1 angular momentum operator, respectively, and are given by

$$\Sigma_z = \begin{pmatrix} 1 & 0 & 0 \\ 0 & 0 & 0 \\ 0 & 0 & -1 \end{pmatrix}, \quad \Sigma_x = \frac{1}{\sqrt{2}} \begin{pmatrix} 0 & 1 & 0 \\ 1 & 0 & 1 \\ 0 & 1 & 0 \end{pmatrix}. \quad (2)$$

If the interactions among the atoms in the BEC are taken into account, in the Hartree approximation, using the single-particle model Hamiltonian, (1), a quasi-1D [3] spinor BEC can be described by the following set of three coupled mean-field partial differential GP equations for the wave-function components ψ_j [2,15,16],

$$i\hbar \frac{\partial \psi_1}{\partial t} = \left(-\frac{\hbar^2}{2m} \frac{\partial^2}{\partial x^2} + V(x) + c_0 \rho \right) \psi_1 + c_2(\rho_1 + \rho_0 - \rho_{-1})\psi_1 + c_2\psi_{-1}^*\psi_0^2 - i\hbar\gamma \frac{\partial \psi_1}{\partial x} + \frac{\Omega}{\sqrt{2}}\psi_0, \quad (3)$$

$$i\hbar \frac{\partial \psi_0}{\partial t} = \left(-\frac{\hbar^2}{2m} \frac{\partial^2}{\partial x^2} + V(x) + c_0 \rho \right) \psi_0 + c_2(\rho_1 + \rho_{-1}) \times \psi_0 + 2c_2\psi_1\psi_{-1}\psi_0^* + \frac{\Omega}{\sqrt{2}}(\psi_1 + \psi_{-1}), \quad (4)$$

$$i\hbar \frac{\partial \psi_{-1}}{\partial t} = \left(-\frac{\hbar^2}{2m} \frac{\partial^2}{\partial x^2} + V(x) + c_0 \rho \right) \psi_{-1} + c_2(\rho_0 + \rho_{-1} - \rho_1)\psi_{-1} + c_2\psi_1^*\psi_0^2 + i\hbar\gamma \frac{\partial \psi_{-1}}{\partial x} + \frac{\Omega}{\sqrt{2}}\psi_0, \quad (5)$$

where $V(x) = m\omega_x^2 x^2/2$ is the 1D harmonic trap, $c_0 = 2\hbar^2(a_0 + 2a_2)/(3ml_{yz}^2)$, $c_2 = 2\hbar^2(a_2 - a_0)/(3ml_{yz}^2)$, a_0 and a_2 are the s -wave scattering lengths in the total spin 0 and 2 channels, respectively, $\rho_j = |\psi_j|^2$ with $j = 1, 0, -1$ are the component densities, $\rho = \sum_{j=-1}^1 |\psi_j|^2$ is the total density, and $l_{yz} = \sqrt{\hbar/(m\omega_{yz})}$ with $\omega_{yz} = \sqrt{\omega_y\omega_z}$ is the oscillator length in the transverse y - z plane. The normalization condition is

$$\int_{-\infty}^{\infty} dx \sum_{j=-1}^1 |\psi_j(x)|^2 = N. \quad (6)$$

In order to transform Eqs. (3)–(5) into dimensionless form, we use the scaled variables, defined as

$$\tilde{t} = \omega_x t, \quad \tilde{x} = \frac{x}{l_0}, \quad \phi_j(\tilde{x}, \tilde{t}) = \frac{\sqrt{l_0}}{\sqrt{N}} \psi_j(\tilde{x}, \tilde{t}), \quad (7)$$

where $l_0 = \sqrt{\hbar/(m\omega_x)}$ is the oscillator length along the x axis and N is the total number of atoms. Using these dimensionless variables, the coupled mean-field Eqs. (3)–(5) in dimensionless form are

$$i \frac{\partial \phi_1}{\partial \tilde{t}} = \left(-\frac{1}{2} \frac{\partial^2}{\partial \tilde{x}^2} + \tilde{V} + \tilde{c}_0 \tilde{\rho} \right) \phi_1 + \tilde{c}_2(\tilde{\rho}_1 + \tilde{\rho}_0 - \tilde{\rho}_{-1})\phi_1 + \tilde{c}_2\phi_{-1}^*\phi_0^2 - i\tilde{\gamma} \frac{\partial \phi_1}{\partial \tilde{x}} + \frac{\tilde{\Omega}}{\sqrt{2}}\phi_0, \quad (8)$$

$$i \frac{\partial \phi_0}{\partial \tilde{t}} = \left(-\frac{1}{2} \frac{\partial^2}{\partial \tilde{x}^2} + \tilde{V} + \tilde{c}_0 \tilde{\rho} \right) \phi_0 + \tilde{c}_2(\tilde{\rho}_1 + \tilde{\rho}_{-1}) \times \phi_0 + 2\tilde{c}_2\phi_1\phi_{-1}\phi_0^* + \frac{\tilde{\Omega}}{\sqrt{2}}(\phi_1 + \phi_{-1}), \quad (9)$$

$$i \frac{\partial \phi_{-1}}{\partial \tilde{t}} = \left(-\frac{1}{2} \frac{\partial^2}{\partial \tilde{x}^2} + \tilde{V} + \tilde{c}_0 \tilde{\rho} \right) \phi_{-1} + \tilde{c}_2(\tilde{\rho}_0 + \tilde{\rho}_{-1} - \tilde{\rho}_1)\phi_{-1} + \tilde{c}_2\phi_1^*\phi_0^2 + i\tilde{\gamma} \frac{\partial \phi_{-1}}{\partial \tilde{x}} + \frac{\tilde{\Omega}}{\sqrt{2}}\phi_0, \quad (10)$$

where $\tilde{V} = \tilde{x}^2/2$, $\tilde{\gamma} = \hbar k_r/(m\omega_x l_0)$, $\tilde{\Omega} = \Omega/(\hbar\omega_x)$, $\tilde{c}_0 = 2N(a_0 + 2a_2)/(3l_{yz}^2)$, $\tilde{c}_2 = 2N(a_2 - a_0)/(3l_{yz}^2)$, $\tilde{\rho}_j = |\phi_j|^2$ with $j = 1, 0, -1$, and $\tilde{\rho} = \sum_{j=-1}^1 |\phi_j|^2$. The normalization condition satisfied by the ϕ_j 's is

$$\int_{-\infty}^{\infty} \sum_{j=-1}^1 \tilde{\rho}_j(\tilde{x}) d\tilde{x} = 1. \quad (11)$$

Another useful quantity related to the component densities—magnetization—is defined by

$$\mathcal{M} = \int_{-\infty}^{\infty} [\tilde{\rho}_1(\tilde{x}) - \tilde{\rho}_{-1}(\tilde{x})] d\tilde{x}. \quad (12)$$

Depending on the value of \tilde{c}_2 (>0 or <0), the system develops interesting physical properties. The interaction in the $5S_{1/2}$ state of ^{87}Rb with $\tilde{c}_2 < 0$ is termed ferromagnetic and that in the $3S_{1/2}$ state of ^{23}Na with $\tilde{c}_2 > 0$ is termed antiferromagnetic or polar. For the sake of simplicity of notations, we represent the dimensionless variables without a tilde in the rest of the paper.

The energy of the spinor BEC in the presence of an SO coupling is [15,16]

$$\begin{aligned}
E = N \int_{-\infty}^{\infty} & \left\{ \frac{1}{2} \left| \frac{d\phi_1}{dx} \right|^2 + \frac{1}{2} \left| \frac{d\phi_0}{dx} \right|^2 + \frac{1}{2} \left| \frac{d\phi_{-1}}{dx} \right|^2 + V\rho \right. \\
& + \frac{c_0}{2} \rho^2 + \frac{c_2}{2} (\rho_1 + \rho_0 - \rho_{-1}) \rho_1 + \frac{c_2}{2} (\rho_1 + \rho_{-1}) \rho_0 \\
& + \frac{c_2}{2} (\rho_0 + \rho_{-1} - \rho_1) \rho_{-1} + c_2 [\phi_{-1}^* \phi_0^2 \phi_1^* \\
& + \phi_{-1} (\phi_0^*)^2 \phi_1] + \gamma \left(-i\phi_1^* \frac{d\phi_1}{dx} + i\phi_{-1}^* \frac{d\phi_{-1}}{dx} \right) \\
& \left. + \frac{\Omega}{\sqrt{2}} (\phi_1^* \phi_0 + \phi_0^* \phi_1 + \phi_{-1}^* \phi_0 + \phi_0^* \phi_{-1}) \right\} dx. \quad (13)
\end{aligned}$$

Based on the form of this energy functional a few inferences about the phase separation among the various components of a spinor BEC with SO coupling can easily be drawn. The energy term proportional to c_0 can never lead to a phase separation, as it contains terms $Nc_0 \int (\rho_j^2/2 + \rho_j \rho_{j'}) dx$, where $j, j' = 1, 0, -1$ and $j \neq j'$, and hence corresponds to a scenario where inter- and intraspecies interactions are of equal strengths. The situation is analogous to a binary BEC with $a_{12}^2 = a_{11}a_{22}$, where a_{11} and a_{22} are intraspecies, and a_{12} interspecies, scattering lengths. Such a binary BEC has equal strengths of inter- and intraspecies nonlinearities and is always miscible in the presence of a 1D harmonic trap [30,33]. Let us now look at the terms proportional to c_2 . For a stable solution, the phases of the three components, say θ_j 's with $j = -1, 0, 1$, should satisfy

$$\theta_1 + \theta_{-1} + s\pi = 2\theta_0, \quad (14)$$

where s is an integer [29,34]. Assuming that $\theta_0 = 0$ and $s = 0$, the interaction energy part of the total energy, (13), can be written as

$$\begin{aligned}
E_{\text{int}} = N \int_{-\infty}^{\infty} & \left\{ \frac{c_0}{2} \rho^2 + \frac{c_2}{2} (\rho_1^2 + \rho_{-1}^2 + 2\rho_1\rho_0 + 2\rho_0\rho_{-1} \right. \\
& \left. - 2\rho_1\rho_{-1} + 4\sqrt{\rho_1\rho_{-1}}\rho_0) \right\} dx. \quad (15)
\end{aligned}$$

The system will naturally move to a state of minimum energy, which could have a phase-separated or an overlapping configuration. A consideration of minimization of energy could reveal whether the system will prefer a ground state with an overlapping or a phase-separated profile.

It is evident from Eq. (15) that in the case of a *ferromagnetic* BEC ($c_2 < 0$), there is only one term, $N \int |c_2| \rho_1 \rho_{-1} dx$, with a positive energy contribution representing interspecies repulsion, which will favor a phase separation between component 1 and component -1 . The minimum contribution from this term can be 0 when components 1 and -1 are fully phase separated, whereas, for the rest of the c_2 -dependent terms in E_{int} , the contribution is always less than 0, representing interspecies attraction. A maximum overlap between the components will reduce the contribution of these terms to the energy. Hence these terms will inhibit a phase separation. So, the phase separation in a ferromagnetic BEC, if ever it occurs, can only take place between component 1 and component -1 .

On the other hand, in the case of a *polar or antiferromagnetic* BEC ($c_2 > 0$), all the terms in Eq. (15) except $-N \int c_2 \rho_1 \rho_{-1} dx$ contribute positive energy, representing interspecies repulsion. For an arbitrary value of magnetization \mathcal{M} , the interaction energy can be minimized in two ways: first, by making $\rho_0 = 0$ and ensuring the maximum overlap between component 1 and component -1 and, second, by fully phase separating the 0th component from the maximally overlapping 1 and -1 components. The interaction energy in both cases becomes

$$E_{\text{int}} = N \int_{-\infty}^{\infty} \left\{ \frac{c_0}{2} \rho^2 + \frac{c_2}{2} (\rho_1^2 + \rho_{-1}^2 - 2\rho_1\rho_{-1}) \right\} dx. \quad (16)$$

Hence, the phase separation in a polar BEC, if it ever occurs, is most likely to take place between the 0th component and overlapping 1 and -1 components.

III. AN SO-COUPLED BEC IN A 1D BOX

To understand the effect of the different terms in the expression for the interaction energy, (15), on phase separation, we study an analytic model of a uniform (trapless) spinor BEC in a 1D box of length $2L$ localized in the region $-L < x < L$. In order to clearly establish the role of the different terms in E_{int} in determining the ground-state structure of the $F = 1$ spinor BEC, first we consider one with zero magnetization ($\mathcal{M} = 0$).

We consider the miscible and immiscible profiles in the case of a ferromagnetic BEC ($c_2 < 0$). In the miscible case, the densities are uniform and written as $\rho_j(x) \equiv n_j$. Because of the symmetry between $j = 1$ and $j = -1$, it is natural to take $n_1 = n_{-1}$. Then the densities of the three components can be written as

$$\rho_1(x) = n_1, \quad -L < x < L, \quad (17)$$

$$\rho_0(x) = n_0, \quad -L < x < L, \quad (18)$$

$$\rho_{-1}(x) = n_{-1} = n_1, \quad -L < x < L. \quad (19)$$

All densities are 0 for $|x| \geq L$. This is the general density distribution for a miscible configuration which we use in this study. In the absence of an SO coupling and Rabi term ($\gamma = \Omega = 0$), the interaction energy, (15), for a ferromagnetic BEC in the 1D box becomes

$$E_{\text{int}} = NL [c_0(4n_1^2 + n_0^2 + 4n_1n_0) - |c_2|8n_1n_0], \quad (20)$$

and the corresponding normalization condition is

$$2L(2n_1 + n_0) = 1. \quad (21)$$

In the trapped case, as considered in Sec. II, the energies, (13) or (15), are extensive properties and increase with the size of the system. However, the energy density (energy per unit length) of a uniform gas, as considered in this section, is an intensive property [30] and does not depend on the system size or the total length of the box, provided that a constant particle density is maintained when the size is changed. Recalling that the constants c_0 and c_2 are proportional to the number of atoms N , Eq. (20), and all other energies in this section reveal the

interesting feature

$$\frac{E_{\text{int}}}{L} \sim \left(\frac{N}{L}\right)^2, \quad (22)$$

also valid for nonspinor systems [30]. The minimum of energy, (20), subject to the normalization constraint, (21), and for n_j 's ≥ 0 , occurs at

$$n_1 = n'_{-1} = \frac{1}{8L}, \quad n_0 = \frac{1}{4L}, \quad (23)$$

and the corresponding minimum energy is

$$E_{\text{int}}^{\text{min(M)}} = N \frac{(c_0 - |c_2|)}{4L}. \quad (24)$$

In the immiscible case, where components $j = 1$ and $j = -1$ are separated, let n'_1 be the density of component 1 from $-L$ to 0 and $n'_{-1} = n'_1$ be the density of component -1 from 0 to L . This symmetric distribution is consistent with the symmetry between component $j = 1$ and component $j = -1$ in the mean-field equations, (8)–(10). The density of component 0 distributed from $-L$ to L is taken to be n'_0 as in the miscible case, so that

$$\rho_1(x) = \begin{cases} n'_1, & -L < x < 0, \\ 0, & 0 \leq x \leq L, \end{cases} \quad (25)$$

$$\rho_0(x) = n'_0, \quad -L < x < L, \quad (26)$$

$$\rho_{-1}(x) = \begin{cases} n'_{-1} = n'_1, & 0 < x < L, \\ 0, & -L \leq x \leq 0. \end{cases} \quad (27)$$

All densities are 0 for $|x| \geq L$. This is the general density distribution for an immiscible configuration, which we use in this study for the ferromagnetic condensate. As mentioned in Sec. II, for a ferromagnetic BEC, a phase separation between the 1 and the -1 components is energetically the most favorable among all possible phase separations. This is the reason to choose the aforementioned distribution for the immiscible profile. The interaction energy for this distribution is

$$E_{\text{int}} = NL[c_0(n_1'^2 + n_0'^2 + 2n_1'n_0') - |c_2|n_1'(n_1' + 2n_0')], \quad (28)$$

with the normalization condition

$$2L(n_1' + n_0') = 1. \quad (29)$$

The condition of the minimum of energy in this case, again subject to the normalization constraint, (29), and for n_j 's ≥ 0 , is

$$n_1' = n'_{-1} = \frac{1}{2L}, \quad n_0' = 0, \quad (30)$$

and the minimum value of the interaction energy $E_{\text{int}}^{\text{min(I)}}$ is the same as in the miscible case, given by Eq. (24): $E_{\text{int}}^{\text{min(M)}} = E_{\text{int}}^{\text{min(I)}}$. Thus, from an energetic consideration, the miscible and immiscible profiles are equally favorable in a homogeneous ferromagnetic BEC in the absence of a confining trap. Now, $n_1' = n'_{-1} = 1/(2L)$ are the maximum density values allowed for these two components of the system with zero magnetization for the immiscible case. Any general distribution with zero magnetization for the immiscible

profile will have, due to the inherent symmetry of the present model between component $j = 1$ and component $j = -1$, $n_1' = 1/(2L) - \delta$ between $x = -L$ and 0, $n'_{-1} = 1/(2L) - \delta$ between $x = 0$ and L , and $n_0' = \delta$ between $x = -L$ and L , with $\delta \geq 0$. The interaction energy corresponding to this general distribution for the immiscible profile is

$$E_{\text{int}} = N \left[\frac{c_0 - |c_2|}{4L} + |c_2|\delta^2 L \right]. \quad (31)$$

Hence, the interaction energy for this immiscible profile is either more than ($\delta > 0$) or equal to ($\delta = 0$) the interaction energy of the miscible one. Hence for a general distribution ($\delta \neq 0$) the miscible profile with the lowest energy will be the preferred ground state. The presence of a trapping potential, however small it may be, will favor the miscible profile due to an extra confining force to the center.

Now let us consider the phase separation in a polar BEC. The interaction energy, (15), can be minimized if we choose

$$n_1 = n_{-1} = \frac{1}{4L}, \quad n_0 = 0 \quad (32)$$

in the case of a miscible profile [viz. Eqs. (17)–(19)] or $n_1 = n_{-1} = 0$, $n_0 = 1/(2L)$ in the case of an immiscible profile [viz. Eqs. (25)–(27)]. This immiscible profile represents effectively a single-component system. The value of the minimum energy in both cases is

$$E_{\text{int}}^{\text{min}} = \frac{Nc_0}{4L}. \quad (33)$$

As mentioned in Sec. II, the phase separation in the polar condensate is most likely to occur between the 0th and overlapping 1 and -1 components. Therefore, we also consider the profile where components 1 and -1 are miscible, and these two are phase separated from the 0th component with the general density distribution

$$\rho_1(x) = \begin{cases} n''_1, & -L < x < -L + L', \\ 0, & -L + L' \leq x \leq L, \end{cases} \quad (34)$$

$$\rho_0(x) = \begin{cases} 0, & -L < x < -L + L', \\ n''_0, & -L + L' \leq x \leq L, \end{cases} \quad (35)$$

$$\rho_{-1}(x) = \begin{cases} n''_{-1} = n''_1, & -L < x < -L + L', \\ 0, & -L + L' \leq x \leq L, \end{cases} \quad (36)$$

where $L' < 2L$, and all the densities are 0 for $|x| > L$. The interaction energy for this distribution is

$$E_{\text{int}} = \frac{Nc_0}{2} [4(n''_1)^2 L' + 2(n''_0)^2 L - (n''_0)^2 L'], \quad (37)$$

with the normalization condition

$$2n''_1 L' + 2n_0 L - n_0 L' = 1. \quad (38)$$

The minimum of this energy, subject to the normalization constraint, occurs at

$$L' = L, \quad n''_1 = n''_{-1} = \frac{1}{4L}, \quad \text{and} \quad n''_0 = \frac{1}{2L}. \quad (39)$$

The minimum interaction energy for this density distribution is the same as for the miscible profile, i.e., $E_{\text{int}}^{\text{min}} = Nc_0/(4L)$. Similarly, it can be shown that for the profile where all three

components are phase separated from each other, as well as the rest of the possible phase-separated profiles, the interaction energy is always greater than $Nc_0/(4L)$ due to a nonzero contribution from the c_2 -dependent terms. So, the energy of any general immiscible profile is either equal to or greater than $Nc_0/(4L)$ due to a nonzero contribution from the c_2 -dependent terms. The presence of a trapping potential, however weak it may be, will make the miscible profile energetically more favorable than all other possible immiscible profiles. Hence, there can be no phase separation in the trapped ferromagnetic and polar BECs.

Next let us consider the effect of SO coupling and the Rabi term on phase separation. First, let us include an SO coupling without the Rabi term ($\gamma \neq 0$, $\Omega = 0$) and discuss the effect on a ferromagnetic BEC ($c_2 < 0$). The presence of this term leads to a constant phase gradient $-\alpha$ and α in ϕ_1 and ϕ_{-1} , respectively [16]. The interaction energy of the miscible profile [viz. Eqs. (17)–(19)] in this case is

$$E_{\text{int}} = NL[c_0(4n_1^2 + n_0^2 + 4n_1n_0) - |c_2|8n_1n_0 + 2\alpha^2n_1 - 4\gamma\alpha n_1], \quad (40)$$

where the $2N\alpha^2n_1L$ term arises from the derivatives of the phases of ϕ_1 and ϕ_{-1} . Minimizing this energy with respect to n_1 and α , subject to the normalization constraint, (21), and $n_j \geq 0$ for $j = 1, 0, -1$, we get

$$\alpha = \gamma, n_1 = \begin{cases} \frac{1}{8L} + \frac{\gamma^2}{16|c_2|}, & \gamma \leq \sqrt{2|c_2|/L}, \\ \frac{1}{4L}, & \gamma > \sqrt{2|c_2|/L}, \end{cases} \quad (41)$$

with the corresponding minimum energy

$$E_{\text{int}}^{\text{min(M)}} = \begin{cases} N\left[\frac{c_0 - |c_2|}{4L} - \frac{\gamma^2}{4} - \frac{L\gamma^4}{16|c_2|}\right], & \gamma \leq \sqrt{2|c_2|/L}, \\ N\left[\frac{c_0}{4L} - \frac{\gamma^2}{2}\right], & \gamma > \sqrt{2|c_2|/L}. \end{cases} \quad (42)$$

The density n_1 of Eq. (41) attains a saturation for $\gamma > \sqrt{2|c_2|/L}$. With further increase in γ the density n_1 does not change, as it has already achieved the maximum permissible density for a state with $\mathcal{M} = 0$ subject to the normalization constraint, (21).

The interaction energy of the immiscible profile [viz. Eqs. (25)–(27)] in this case is

$$E_{\text{int}} = NL[c_0(n_1'^2 + n_0'^2 + 2n_1'n_0') - |c_2|n_1'(n_1' + 2n_0') + \alpha'^2n_1' - 2\gamma\alpha'n_1'], \quad (43)$$

Minimizing this energy with respect to n_1' and α' , subject to the normalization constraint, (29), and $n_j \geq 0$ for $j = 1, 0, -1$, we get

$$\alpha' = \gamma, \quad n_1' = \frac{1}{2L}, \quad (44)$$

with the corresponding minimum energy

$$E_{\text{int}}^{\text{min(I)}} = N\left[\frac{c_0 - |c_2|}{4L} - \frac{\gamma^2}{2}\right]. \quad (45)$$

Comparing Eqs. (42) and (45), we find that the immiscible profile has a lower energy than the miscible one for any nonzero value of γ for a ferromagnetic BEC: $E_{\text{int}(\Omega)}^{\text{min(I)}} < E_{\text{int}(\Omega)}^{\text{min(M)}}$. Hence

the SO coupling will favor phase separation in a ferromagnetic BEC.

Let us now discuss phase separation in a polar BEC in the presence of SO coupling. The interaction energy of the miscible profile [viz. Eqs. (17)–(19)] in this case is

$$E_{\text{int}} = NL[c_0(4n_1^2 + n_0^2 + 4n_1n_0) + 8c_2n_1n_0 + 2\alpha^2n_1 - 4\gamma\alpha n_1]. \quad (46)$$

Minimizing it, subject to the normalization constraint, (21), and $n_j \geq 0$, we get

$$\alpha = \gamma, \quad n_1 = n_{-1} = \frac{1}{4L}, \quad n_0 = 0. \quad (47)$$

The value of the minimum energy for this miscible profile is

$$E_{\text{int}}^{\text{min(M)}} = N\left[\frac{c_0}{4L} - \frac{\gamma^2}{2}\right]. \quad (48)$$

Similarly, the energy of the immiscible profile [viz. Eqs. (25)–(27)] of the polar BEC is

$$E_{\text{int}} = NL[c_0(n_1'^2 + n_0'^2 + 2n_1'n_0') + c_2n_1'(n_1' + 2n_0') + \alpha'^2n_1' - 2\gamma\alpha'n_1']. \quad (49)$$

Minimizing this energy, subject to the normalization constraint, (29), and $n_j \geq 0$, we get

$$n_1' = n_{-1}' = \begin{cases} \frac{1}{2L}, & \gamma > \sqrt{c_2/(2L)}, \\ 0, & \gamma \leq \sqrt{c_2/(2L)}, \end{cases} \quad (50)$$

with the corresponding minimum energy given by

$$E_{\text{int}}^{\text{min(I)}} = \begin{cases} N\left[\frac{c_0 + c_2}{4L} - \frac{\gamma^2}{2}\right], & \gamma > \sqrt{c_2/(2L)}, \\ \frac{Nc_0}{4L}, & \gamma \leq \sqrt{c_2/(2L)}. \end{cases} \quad (51)$$

This energy is higher than the energy of the miscible profile given by Eq. (48): $E_{\text{int}}^{\text{min(I)}} > E_{\text{int}}^{\text{min(M)}}$. Similarly, it can be argued that the energies of the other possible immiscible profiles with $n_0 \neq 0$, like the distribution in Eqs. (34)–(36), are always higher than $N(c_0 - 2\gamma^2L)/(4L)$ due to the increase in the negative energy contribution from the γ -dependent term; i.e., this contribution is larger than $-\gamma^2/2$. Hence, the SO coupling will favor miscibility in the case of a polar BEC.

Now let us analyze the role of the Rabi term ($\Omega \neq 0$). For the sake of simplicity let us assume that $\gamma = 0$. The energy contribution from the Rabi term is

$$E_{\text{int}(\Omega)} = \sqrt{2\rho_0(x)}\Omega N \int_{-\infty}^{\infty} [\sqrt{\rho_1(x)}\cos(\theta_0 - \theta_1) + \sqrt{\rho_{-1}(x)}\cos(\theta_0 - \theta_{-1})]dx. \quad (52)$$

This expression is valid for nonuniform densities in general, and not just in the case of uniform densities appropriate for the 1D box. This term will lead to a decrease in the energy of the system if

$$\frac{\pi}{2} < |\theta_0 - \theta_1| < \frac{3\pi}{2} \quad \text{and} \quad \frac{\pi}{2} < |\theta_0 - \theta_{-1}| < \frac{3\pi}{2}. \quad (53)$$

Assuming that $\theta_0 = 0$, the minimum of $E_{\text{int}(\Omega)}$ for the miscible profile [viz. Eqs. (17)–(19)] occurs at

$$n_1 = n_{-1} = \frac{1}{8L}, \quad n_0 = \frac{1}{4L}, \quad |\theta_1| = |\theta_{-1}| = \pi. \quad (54)$$

The value of the corresponding minimum energy is $E_{\text{int}(\Omega)}^{\text{min}(M)} = -N\Omega$. The minimum for the immiscible profile [viz. Eqs. (25)–(27)] occurs at

$$n_1 = n_{-1} = \frac{1}{4L}, \quad n_0 = \frac{1}{4L}, \quad |\theta_1| = |\theta_{-1}| = \pi, \quad (55)$$

with the corresponding energy minimum $E_{\text{int}(\Omega)}^{\text{min}(I)} = -N\Omega/\sqrt{2}$. Also, the $E_{\text{int}(\Omega)}$ of the distribution represented by Eqs. (34)–(36) is uniformly 0 and hence greater than $-N\Omega$. Hence, the Rabi term favors miscibility in the spinor BEC irrespective of the nature of the spin interaction: ferromagnetic or polar. It implies that in a ferromagnetic BEC the terms containing γ (favoring phase separation) and Ω (favoring miscibility) will have opposite roles as far as phase separation is concerned.

IV. A SPINOR BEC IN A HARMONIC TRAP

In the presence of a harmonic trap, we study the ground-state structure of the spinor BEC by solving Eqs. (8)–(10) numerically. We use the split-time-step finite-difference method to solve the coupled equations, (8)–(10) [15,35]. The spatial and time steps employed in the present work are $\delta x = 0.05$ and $\delta t = 0.000125$. In order to find the ground state, we solve Eqs. (8)–(10) by imaginary-time propagation. The imaginary time propagation conserves neither the norm nor magnetization. To fix both the norm and magnetization, we use the method reported in Ref. [16]. Accordingly, after each iteration in imaginary time $\tau = -it$, the wave-function components are transformed as

$$\phi_j(x, \tau + d\tau) = d_j \phi_j(x, \tau), \quad (56)$$

where d_j 's with $j = 1, 0, -1$ are the normalization constants. Now the chemical potentials of the three components are related as

$$\mu_1 + \mu_{-1} = 2\mu_0. \quad (57)$$

Using this relation, one can derive the relation among the three normalization constants [16]:

$$d_1 d_{-1} = d_0^2. \quad (58)$$

Using Eq. (58) along with the normalization [viz. Eq. (6)] and magnetization constraints [viz. Eq. (12)], d_j 's can be determined as [16]

$$d_0 = \frac{\sqrt{1 - \mathcal{M}^2}}{\sqrt{N_0 + \sqrt{4(1 - \mathcal{M}^2)N_1 N_{-1} + \mathcal{M}^2 N_0^2}}}, \quad (59)$$

$$d_1 = \sqrt{\frac{1 + \mathcal{M} - c_0^2 N_0}{2N_1}}, \quad (60)$$

$$d_{-1} = \sqrt{\frac{1 - \mathcal{M} - c_0^2 N_0}{2N_{-1}}}, \quad (61)$$

and here $N_j = \int |\phi_j(x, \tau)|^2 dx$. These normalization constants ensure that the norm and magnetization are both conserved after each iteration in imaginary time. The quasi-1D trap considered here has $\omega_x = 2\pi \times 20$ Hz and $\omega_y = \omega_z = 2\pi \times 400$ Hz. We consider ^{87}Rb atoms with $a_0 = 5.387$ nm and

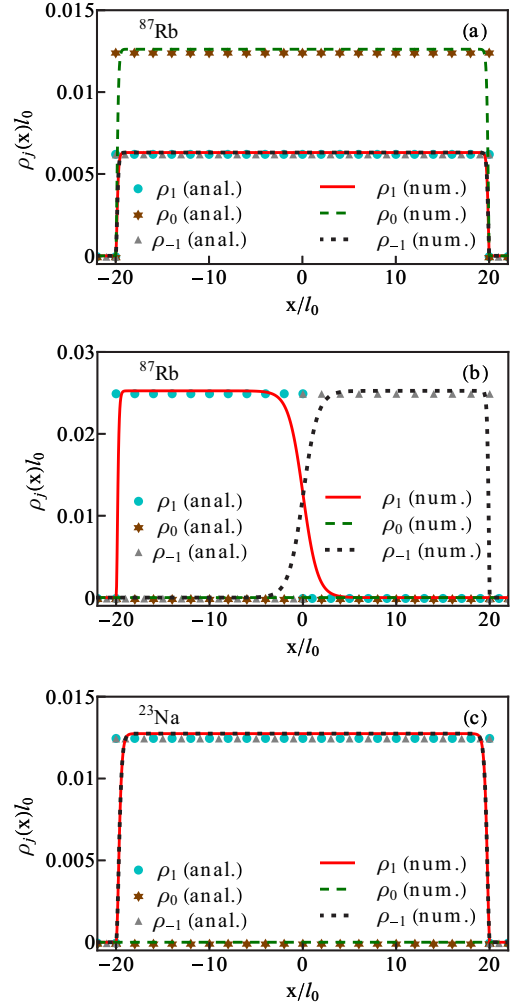


FIG. 1. (Color online) (a, b) Analytical (anal.) and numerical (num.) densities $\rho_j(x)l_0$ of a condensate of ^{87}Rb atoms with $c_0 = 885.72l_0$ and $c_2 = -4.09l_0$ in a 1D box of length $40l_0$. The SO coupling $\gamma = 0$ and 0.5 for (a) and (b), respectively. (c) The same for a condensate of ^{23}Na atoms with $c_0 = 241.28l_0$ and $c_2 = 7.76l_0$ in the presence of an arbitrary SO coupling. Both the densities and the spatial coordinates are in dimensionless units.

$a_2 = 5.313$ nm as a typical example of a ferromagnetic BEC. As a polar BEC, we consider ^{23}Na , which has $a_0 = 2.646$ nm and $a_2 = 2.911$ nm. The values of l_0 are 2.41 and $4.69 \mu\text{m}$ for ^{87}Rb and ^{23}Na , respectively.

Before proceeding to the numerical solutions for the spinor condensate in a harmonic trap, let us first compare the analytic results for the condensate in a 1D box with the corresponding numerical ones. For this purpose, we consider the aforementioned oscillator lengths for ^{87}Rb and ^{23}Na in a 1D box of length $40l_0$. The nonlinearities (c_0, c_2) considered for ^{87}Rb and ^{23}Na are, respectively, $(885.72l_0, -4.09l_0)$ and $(241.28l_0, 7.76l_0)$. In Fig. 1(a), analytic and numerical densities for the ^{87}Rb condensate in the absence of SO coupling and the Rabi term, given by Eq. (23), are plotted. In Fig. 1(b), analytic and numerical densities for the ^{87}Rb condensate in the presence of SO coupling ($\gamma = 0.5, \Omega = 0$), given by Eq. (44), are shown. Finally, in Fig. 1(c), the same for the ^{23}Na

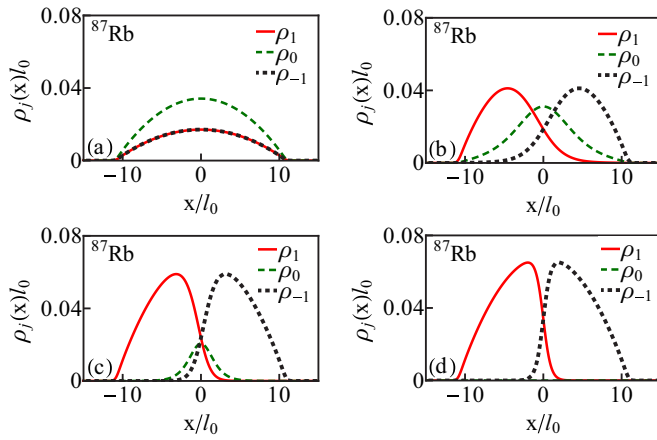


FIG. 2. (Color online) Ground-state structure of an ^{87}Rb spinor BEC with 10 000 atoms with $\Omega = 0$. The SO coupling $\gamma = 0, 0.25, 0.5, 1$ for (a), (b), (c), and (d), respectively. All quantities are in dimensionless units.

condensate in the absence as well as the presence of an arbitrary SO coupling, given by Eqs. (32) and (47), are illustrated. We find that the numerical results are in good agreement with the analytic predictions as shown in Fig. 1.

Now let us discuss harmonically trapped spinor condensates. In Fig. 2 we present the densities of the ground state of 10 000 ^{87}Rb atoms with different SO couplings and without the Rabi term. Without SO coupling, the ground-state solution for ^{87}Rb is miscible and $\rho_0(x) > \rho_1(x) = \rho_{-1}(x)$ for zero magnetization ($\mathcal{M} = 0$) [viz. Fig. 2(a)], which is in qualitative agreement with the conclusion of the analytic study of the uniform system in Sec. III given by Eq. (23). If the number of atoms is sufficiently large, as the SO coupling γ is increased, the density ρ_0 starts decreasing slowly, which ultimately makes the system immiscible as shown in Figs. 2(a)–2(d). For a sufficiently strong SO coupling, ρ_0 becomes 0 and there is a maximum of phase separation between the two remaining component densities, $\rho_1(x)$ and $\rho_{-1}(x)$. This is, again, in agreement with the result of the analytic study on the uniform system given by Eq. (44), which predicts zero density for the 0th component. However, if the number of atoms is smaller ($N \leq 1000$), the 0th component again vanishes with an increase in the SO coupling γ above a critical value, but there is no phase separation between component 1 and component -1 .

The state with $\rho_0(x) = 0$ appears naturally with an increase in the SO coupling, and in a zero-magnetization case this guarantees an equal number of atoms for components 1 and -1 , resulting in $\rho_1(x) = \rho_{-1}(-x)$. It is interesting to study the fate of this state as the magnetization is increased ($\mathcal{M} > 0$). Keeping $\gamma = 1$ and $\Omega = 0$ fixed, one can change the relative proportion of ρ_1 and ρ_{-1} by changing the magnetization \mathcal{M} , as shown in Figs. 3(a)–3(d), maintaining $\rho_0(x) = 0$. With increasing \mathcal{M} the relative density of component -1 decreases and the system changes from immiscible to miscible.

We have also studied the effect of an increase in the Rabi term Ω on a state with $\rho_0(x) = 0$ [viz. Fig. 2(d)], maintaining magnetization $\mathcal{M} = 0$. As discussed in Sec. III, the Rabi term Ω favors miscibility of the system irrespective of the nature of

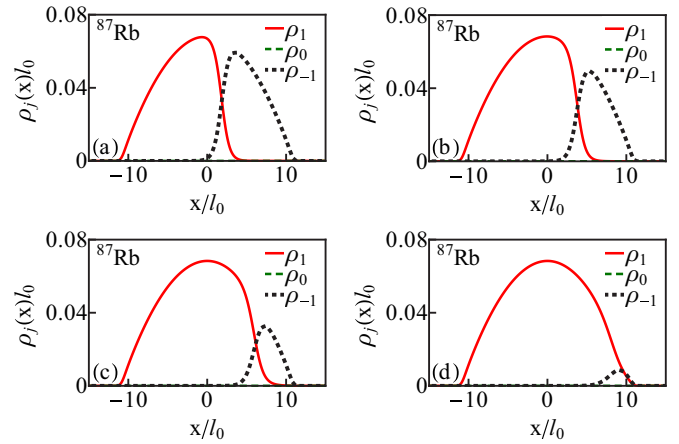


FIG. 3. (Color online) Ground-state structure of an ^{87}Rb spinor BEC with 10 000 atoms and $\Omega = 0$, $\gamma = 1$. Both the density and the spatial coordinates are plotted in dimensionless units. The magnetization $\mathcal{M} = 0.25, 0.5, 0.75$, and 0.95 for (a), (b), (c), and (d), respectively.

the spin-dependent interactions, while the SO-coupling term γ favors a phase separation. Hence, when both γ and Ω are nonzero, there is competition between these two terms, as one favors phase separation, whereas the other favors miscibility. To illustrate this, in Figs. 4(a) and 4(b) we plot the component densities for $\Omega = 0.1$ and 1 , respectively, for $N = 10\,000$ and $\gamma = 1$. The increase in the Rabi term Ω from 0.1 to 1 has transformed a phase-separated state to a miscible state. For a smaller number of atoms, say $N = 1000$, we do not observe any phase separation with the increase in the SO coupling γ . Nevertheless, the increase in γ leads to a decrease in ρ_0 as shown in Fig. 4(c), where ρ_0 is negligible in comparison to overlapping ρ_1 and ρ_{-1} . Again, as Ω is increased in this case, the density ρ_0 first increases and ultimately ends up being higher than those of the other two components [viz. Fig. 4(d)].

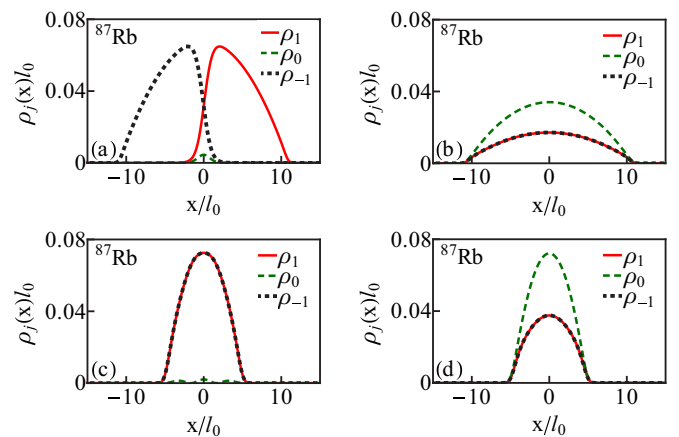


FIG. 4. (Color online) Ground-state structure of an ^{87}Rb spinor BEC with 10^4 atoms with (a) $N = 10\,000$, $\Omega = 0.1$, $\gamma = 1$; (b) $N = 10\,000$, $\Omega = 1$, $\gamma = 1$; (c) $N = 1000$, $\Omega = 0.1$, $\gamma = 1$; and (d) $N = 1000$, $\Omega = 1$, $\gamma = 1$. Both the density and the spatial coordinates are plotted in dimensionless units. The magnetization $\mathcal{M} = 0$ in all the cases.

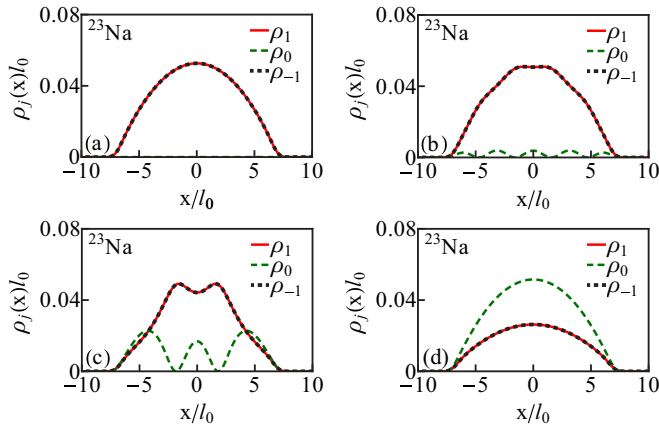


FIG. 5. (Color online) Ground-state structure of a ^{23}Na spinor BEC with (a) $N = 10000$, $\Omega = 0$, $\gamma = 1$ and, also, $\gamma = 0$; (b) $N = 10000$, $\Omega = 0.5$, $\gamma = 1$; (c) $N = 10000$, $\Omega = 1$, $\gamma = 1$; and (d) $N = 10000$, $\Omega = 1.5$, $\gamma = 1$. Both the density and the spatial coordinates are plotted in dimensionless units. The magnetization $\mathcal{M} = 0$ is 0 in all cases.

In the case of the SO-coupled polar BEC ^{23}Na , we do not observe any phase separation, consistent with the discussion of the uniform BEC in Sec. III. In the absence of the Rabi term ($\Omega = 0$), the density profile in the presence and absence of SO coupling are the same as shown in Fig. 5(a). The introduction of the Rabi term leads to a nonzero density of the 0th component as shown in Fig. 5(b) for $\Omega = 0.5$. For both ferromagnetic and polar BECs, in the presence of both SO coupling and Rabi terms, we observe the formation of structure in the ground

state, where the 0th component develops a train of dark notches as shown in Fig. 4(c) for ^{87}Rb and Figs. 5(b) and 5(c) for ^{23}Na . In ^{23}Na , an increase in the Rabi term Ω leads to an increase in $\rho_0(x)$ from 0, at the cost of $\rho_1(x)$ and $\rho_{-1}(x)$ as in the case of ^{87}Rb , and, ultimately, ends up with a solution where $\rho_0(x) > \rho_1(x) = \rho_{-1}(x)$.

V. SUMMARY

We have studied SO-coupled $F = 1$ spinor BECs of ^{87}Rb (ferromagnetic) and ^{23}Na (antiferromagnetic or polar) atoms in quasi-1D traps. By comparing the energies of various competing structures for the SO-coupled spinor BEC in a 1D box, we have shown that any nonzero value of SO coupling will lead to a phase separation between the $m_F = 1$ and the $m_F = -1$ components in the case of a ferromagnetic BEC in the absence of the Rabi term. On the other hand, for a polar BEC, SO coupling makes the miscible profile energetically more stable compared to various possible phase-separated profiles. In the case of trapped SO-coupled BECs, we have numerically studied the ground-state structures. In the ferromagnetic case, above a critical number of atoms the BEC phase separates if the SO coupling strength exceeds a critical value in the absence of the Rabi term. The introduction of the Rabi term favors miscibility for both ferromagnetic and polar BECs. The present conclusions can be tested in experiments with present-day technology.

ACKNOWLEDGMENTS

This work was financed by FAPESP (Brazil) under Contract No. 2013/07213-0 and also supported by CNPq (Brazil).

-
- [1] D. M. Stamper-Kurn, M. R. Andrews, A. P. Chikkatur, S. Inouye, H.-J. Miesner, J. Stenger, and W. Ketterle, *Phys. Rev. Lett.* **80**, 2027 (1998).
- [2] Y. Kawaguchi and M. Ueda, *Phys. Rep.* **520**, 253 (2012).
- [3] L. Salasnich, A. Parola, and L. Reatto, *Phys. Rev. A* **65**, 043614 (2002).
- [4] T. Ohmi and K. Machida, *J. Phys. Soc. Jpn.* **67**, 1822 (1998).
- [5] T. L. Ho, *Phys. Rev. Lett.* **81**, 742 (1998).
- [6] J. Higbie and D. M. Stamper-Kurn, *Phys. Rev. Lett.* **88**, 090401 (2002); T. L. Ho and S. Zhang, *ibid.* **107**, 150403 (2011); Y. Deng, J. Cheng, H. Jing, C. P. Sun, and S. Yi, *ibid.* **108**, 125301 (2012); J. Radic, T. A. Sedrakyan, I. B. Spielman, and V. Galitski, *Phys. Rev. A* **84**, 063604 (2011).
- [7] Y. A. Bychkov and E. I. Rashba, *J. Phys. C* **17**, 6039 (1984).
- [8] G. Dresselhaus, *Phys. Rev.* **100**, 580 (1955).
- [9] X.-J. Liu, M. F. Borunda, X. Liu, and J. Sinova, *Phys. Rev. Lett.* **102**, 046402 (2009).
- [10] Y.-J. Lin, K. Jiménez-García, and I. B. Spielman, *Nature* **471**, 83 (2011).
- [11] V. Galitski and I. B. Spielman, *Nature* **494**, 49 (2013).
- [12] J.-Y. Zhang, S.-C. Ji, Z. Chen, L. Zhang, Z.-D. Du, B. Yan, G.-S. Pan, B. Zhao, Y.-J. Deng, H. Zhai, S. Chen, and J.-W. Pan, *Phys. Rev. Lett.* **109**, 115301 (2012); C. Qu, C. Hamner, M. Gong, C. Zhang, and P. Engels, *Phys. Rev. A* **88**, 021604(R) (2013); M. Aidelsburger, M. Atala, S. Nascimbene, S. Trotzky, Y. A. Chen, and I. Bloch, *Phys. Rev. Lett.* **107**, 255301 (2011); Z. Fu, P. Wang, S. Chai, L. Huang, and J. Zhang, *Phys. Rev. A* **84**, 043609 (2011).
- [13] G. Juzeliūnas, J. Ruseckas, and J. Dalibard, *Phys. Rev. A* **81**, 053403 (2010); J. Dalibard *et al.*, *Rev. Mod. Phys.* **83**, 1523 (2011).
- [14] P. Wang, Z.-Q. Yu, Z. Fu, J. Miao, L. Huang, S. Chai, H. Zhai, and J. Zhang, *Phys. Rev. Lett.* **109**, 095301 (2012); L. W. Cheuk, A. T. Sommer, Z. Hadzibabic, T. Yefsah, W. S. Bakr, and M. W. Zwierlein, *ibid.* **109**, 095302 (2012).
- [15] H. Wang, *Int. J. Comput. Math.* **84**, 925 (2007).
- [16] W. Bao and F. Y. Lim, *SIAM J. Sci. Comp.* **30**, 1925 (2008); F. Y. Lim and W. Bao, *Phys. Rev. E* **78**, 066704 (2008).
- [17] C. Wang, C. Gao, C.-M. Jian, and H. Zhai, *Phys. Rev. Lett.* **105**, 160403 (2010); A. Aftalion and P. Mason, *Phys. Rev. A* **88**, 023610 (2013); R. Gupta, G. S. Singh, and J. Bosse, *ibid.* **88**, 053607 (2013); Q.-Q. Lu and D. E. Sheehy, *ibid.* **88**, 043645 (2013).
- [18] T. D. Stanescu, B. Anderson, and V. Galitski, *Phys. Rev. A* **78**, 023616 (2008); C.-J. Wu, I. Mondragon-Shem, and X.-F. Zhou, *Chin. Phys. Lett.* **28**, 097102 (2011); Q. Zhou and X. Cui, *Phys. Rev. Lett.* **110**, 140407 (2013); S. Gopalakrishnan, A. Lamacraft, and P. M. Goldbart, *Phys. Rev. A* **84**, 061604(R) (2011); H. Hu, B. Ramachandran, H. Pu, and X.-J. Liu, *Phys. Rev. Lett.* **108**, 010402 (2012); B. Ramachandran, B. Opanchuk,

- X.-J. Liu, H. Pu, P. D. Drummond, and H. Hu, *Phys. Rev. A* **85**, 023606 (2012); S. Sinha, R. Nath, and L. Santos, *Phys. Rev. Lett.* **107**, 270401 (2011); T. Ozawa and G. Baym, *Phys. Rev. A* **85**, 013612 (2012).
- [19] Z. F. Xu, Y. Kawaguchi, L. You, and M. Ueda, *Phys. Rev. A* **86**, 033628 (2012); S.-W. Song, Y.-C. Zhang, H. Zhao, X. Wang, and W.-M. Liu, *ibid.* **89**, 063613 (2014); P.-S. He, Y.-H. Zhu, and W.-M. Liu, *ibid.* **89**, 053615 (2014); Y. Deng, J. Cheng, H. Jing, and S. Yi, *Phys. Rev. Lett.* **112**, 143007 (2014); K. Riedl, C. Drukier, P. Zalom, and P. Kopietz, *Phys. Rev. A* **87**, 063626 (2013); T. Kawakami, T. Mizushima, and K. Machida, *ibid.* **84**, 011607 (2011); Z. F. Xu, R. Lü, and L. You, *ibid.* **83**, 053602 (2011); S.-K. Yip, *ibid.* **83**, 043616 (2011); S.-W. Su, I.-K. Liu, Y.-C. Tsai, W. M. Liu, and S.-C. Gou, *ibid.* **86**, 023601 (2012); Y. Zhang, L. Mao, and C. Zhang, *Phys. Rev. Lett.* **108**, 035302 (2012); S.-W. Song, Y.-C. Zhang, L. Wen, and H. Wang, *J. Phys. B* **46**, 145304 (2013).
- [20] E. Ruokokoski, J. A. M. Huhtamäki, and M. Möttönen, *Phys. Rev. A* **86**, 051607(R) (2012).
- [21] J. Larson, J.-P. Martikainen, A. Collin, and E. Sjöqvist, *Phys. Rev. A* **82**, 043620 (2010).
- [22] M. Merkl, A. Jacob, F. E. Zimmer, P. Öhberg, and L. Santos, *Phys. Rev. Lett.* **104**, 073603 (2010).
- [23] T. Ozawa, L. P. Pitaevskii, and S. Stringari, *Phys. Rev. A* **87**, 063610 (2013); D. W. Zhang, J. P. Chen, C. J. Shan, Z. D. Wang, and S. L. Zhu, *ibid.* **88**, 013612 (2013); Q. Zhu, C. Zhang, and B. Wu, *Europhys. Lett.* **100**, 50003 (2012); D. Toniolo and J. Linder, *Phys. Rev. A* **89**, 061605(R) (2014).
- [24] M. A. Garcia-March, G. Mazzarella, L. Dell'Anna, B. Juliá-Díaz, L. Salasnich, and A. Polls, *Phys. Rev. A* **89**, 063607 (2014).
- [25] A. L. Fetter, *Phys. Rev. A* **89**, 023629 (2014); X. F. Zhou, J. Zhou, and C. Wu, *ibid.* **84**, 063624 (2011); Z.-F. Xu, S. Kobayashi, and M. Ueda, *ibid.* **88**, 013621 (2013); C.-F. Liu, Y.-M. Yu, S.-C. Gou, and W.-M. Liu, *ibid.* **87**, 063630 (2013).
- [26] H. Sakaguchi, B. Li, and B. A. Malomed, *Phys. Rev. E* **89**, 032920 (2014); Y. Xu, Y. Zhang, and B. Wu, *Phys. Rev. A* **87**, 013614 (2013); O. Fialko, J. Brand, and U. Zulicke, *ibid.* **85**, 051605(R) (2012).
- [27] F. Zhou, *Phys. Rev. Lett.* **87**, 080401 (2001); S. Yi, Ö. E. Müstecaplioglu, C. P. Sun, and L. You, *Phys. Rev. A* **66**, 011601(R) (2002); W. Zhang, S. Yi, and L. You, *New J. Phys.* **5**, 77 (2003); K. Murata, H. Saito, and M. Ueda, *Phys. Rev. A* **75**, 013607 (2007).
- [28] M. Matuszewski, T. J. Alexander, and Y. S. Kivshar, *Phys. Rev. A* **80**, 023602 (2009).
- [29] M. Matuszewski, *Phys. Rev. A* **82**, 053630 (2010).
- [30] P. Ao and S. T. Chui, *Phys. Rev. A* **58**, 4836 (1998); P. Facchi, G. Florio, S. Pascazio, and F. V. Pepe, *J. Phys. A: Math. Theor.* **44**, 505305 (2011).
- [31] Z. Lan and P. Öhberg, *Phys. Rev. A* **89**, 023630 (2014).
- [32] Y. Li, G. I. Martone, L. P. Pitaevskii, and S. Stringari, *Phys. Rev. Lett.* **110**, 235302 (2013); Y. Zhang and C. Zhang, *Phys. Rev. A* **87**, 023611 (2013); L. Salasnich and B. A. Malomed, *ibid.* **87**, 063625 (2013); D. A. Zezyulin, R. Driben, V. V. Konotop, and B. A. Malomed, *ibid.* **88**, 013607 (2013); Y. Cheng, G. Tang, and S. K. Adhikari, *ibid.* **89**, 063602 (2014).
- [33] S. Gautam and D. Angom, *J. Phys. B* **44**, 025302 (2011); **43**, 095302 (2010).
- [34] T. Isoshima, K. Machida, and T. Ohmi, *J. Phys. Soc. Jpn.* **70**, 1604 (2001).
- [35] P. Muruganandam and S. K. Adhikari, *Comput. Phys. Commun.* **180**, 1888 (2009); D. Vudragovic, I. Vidanovic, A. Balaz, P. Muruganandam, and S. K. Adhikari, *ibid.* **183**, 2021 (2012).